



**The 15<sup>th</sup> ISAV2025**  
**International Conference on**  
**Acoustics and Vibration**  
24-25 Dec 2025      Tehran- Iran

## **Implementation of a Precise Vibration Measurement System Based on Michelson Interferometer**

Morteza Joorablue<sup>a,b\*</sup>, Masoumeh Feyzian<sup>a,c</sup>, Seyed Roohollah Hosseini<sup>a,d</sup>, Hamidreza Safari<sup>a,e</sup>

<sup>a</sup> Arman Moj Fanavar Co., Tehran, Iran

<sup>b</sup> Department of Electrical Engineering, Sharif University of Technology, Tehran, Iran.

<sup>c</sup> Department of Physics, Iran University of Science and Technology, Tehran, Iran.

<sup>d</sup> Department of Physics, University of Tehran, Tehran, Iran.

<sup>e</sup> School of Physics, Institute for Research in Fundamental Sciences (IPM), Tehran, Iran.

\* Corresponding author e-mail: [joorablue@gmail.com](mailto:joorablue@gmail.com)

### **Abstract**

In this paper, we present a system for precise vibration measurement of mechanical structures using a Michelson interferometer. The system was employed to detect nanometer-scale vibrations in a mirror induced by a speaker attached to it, with analysis performed in both time and frequency domains. It successfully measured the frequency of single-tone vibrations with an accuracy of a few hertz, even when the mirror was positioned several meters away. To estimate the resonant frequency of a mechanical structure, we applied an impulse input and transformed the resulting vibration signals using Fast Fourier Transform (FFT). The estimated resonance was validated by applying single-tone inputs at various frequencies, including those near the predicted resonance. As a demonstration of the system's sensitivity and for educational purposes, we played music through the speaker attached to the mirror, and the system was able to reproduce the original audio from the detected vibrations. Finally, we used the setup to measure vibrations generated by an electric motor in a linear guide system, where the mirror was attached to the movable platform.

---

**Keywords:** Vibration; Michelson interferometer; Implementation; Precision measurement.

---

## 1. Introduction

Precise vibration measurement plays a critical role in monitoring the stability and proper functioning of mechanical systems. Faults or instabilities in such systems often manifest as abnormal vibration patterns; for example, a bridge may exhibit unusual vibrations long before structural failure occurs [1]. In high-precision applications, even the slightest vibrations can compromise system performance. For instance, in electron microscopes, where high resolution is essential, the accuracy of measurements depends heavily on the stability of the electron beam, which can be disrupted by nanometer-scale vibrations [2]. Optical interferometry has been a cornerstone technique in vibrometry for several decades, enabling highly precise vibration measurements with sub-nanometer, and in some cutting-edge systems, even picometer resolution [3]. A Michelson interferometer is an optical interferometer used in this paper to perform vibrometry. Fig. 1(a) shows the setup for a simple Michelson interferometer. In this setup, the light coming out of the laser, passes through a lens and is split into two coherent beams at beam splitter. Each beam is reflected back from one of the two mirrors (M1 and M2) and recombined at the beam splitter, producing an interference pattern that is projected onto a screen, as illustrated in Fig. 1(b).

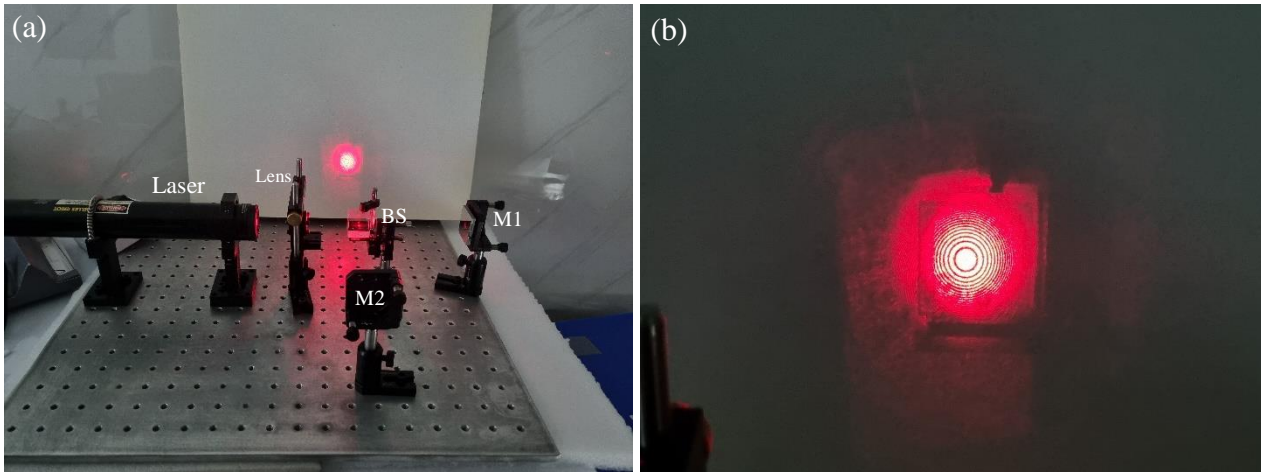


**Figure 1.** (a). Setup of a simple Michelson interferometer (b). Interference pattern

The difference in the distances between the mirrors and the beam splitter determines the optical path length difference between the two beams which in turn affects the phase difference between the two beams. When the beams are in phase, they interfere constructively resulting a bright spot at the center of the pattern; when they are out of phase, they interfere destructively producing a dark spot in the center. Therefore if one of the mirrors are slightly moved, the phase difference between the two beams and therefore the intensity of light changes, this enables us to measure the small mirror vibration by monitoring the changes of light intensity at the interference pattern. The relationship between the phase difference and the displacement of one of the mirrors is given by [4]:

$$\Delta\varphi = 2\pi \frac{2d}{\lambda} \quad (1)$$

Where  $d$  is the mirror displacement,  $\lambda$  is the laser wavelength and  $\Delta\varphi$  is the resulting phase difference. This relation indicates that a displacement in order of a fraction of  $\lambda$ , which is around 632.8nm for the laser we used, can change the phase difference and therefore the light intensity in the interference pattern noticeably. This sensitivity enables the detection of vibrations in nanometer range in the mirror.

## 2. Methodology

The interference intensity as a function of mirror displacement is given by [4]:

$$I(d) = 2I_0(1 + \cos(2\pi \frac{2d}{\lambda})) \quad (2)$$

Where  $I_0$  is the intensity of each beam and  $I$  is the intensity of light due to interference. Therefore as Fig.2 illustrates,  $I$  is a sinusoid function of  $d$ .

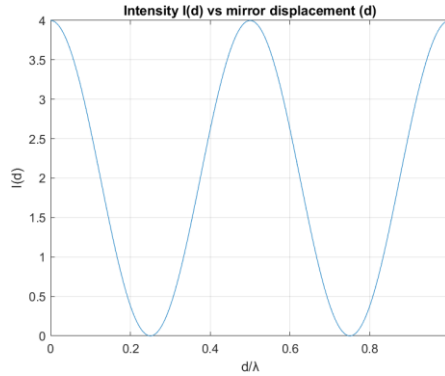


**Figure 2.** Intensity  $I(d)$  vs displacement  $d$  (Normalised to wavelength)

To find the effect of vibration on light intensity, we assume that the mirror is vibrating around a fixed point  $d = d_0$  and the vibration is a function of time  $\delta(t)$  therefore the displacement of the mirror is a function of time and written as

$$d(t) = d_0 + \delta(t); \quad (3)$$

By substituting that in Eq. (2) we have

$$I(t) = 2I_0(1 + \cos(\frac{4\pi d_0}{\lambda} + 4\pi \frac{\delta(t)}{\lambda})) \quad (4)$$

For small vibrations ( $\delta(t) \ll \lambda$ ), a first order approximation yields

$$I(t) \approx 2I_0(1 + \cos(\frac{4\pi d_0}{\lambda})) - \sin(\frac{4\pi d_0}{\lambda}) 4\pi \frac{\delta(t)}{\lambda} \quad (5)$$

Therefore, for small vibrations,  $I(t)$  is a linear function of  $\delta(t)$ . Fig. 3 (a) and (b) show intensity of light for a small and a large harmonic vibration. When the vibration is small,  $I(t)$  is approximately a sinusoid but when the vibration is large, the response is not linear and distortion occurs.

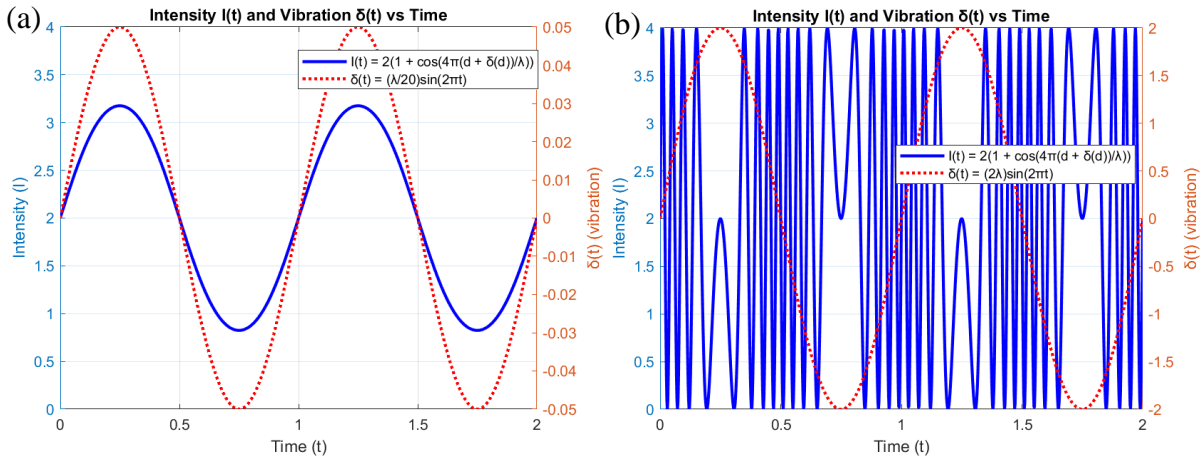


**Figure 3.** Intensity  $I(t)$  and vibration vs time for a harmonic vibration  $\delta(t) = A\sin(2\pi t)$  with  $d_0 = 3\lambda/8$

(a).  $A = \frac{\lambda}{20}$ : response is approximately linear    (b).  $A = 2\lambda$ : response is distorted

For vibrations smaller than  $\lambda/20$ , the change in light intensity is proportional to the mirror's displacement. Therefore, the vibration amplitude can be determined by measuring the corresponding change in light intensity. In this paper, we apply this method to detect vibrations with amplitudes less than  $\lambda/20$  which corresponds to approximately 30 nm (60nm peak to peak) for the helium–neon laser used

in our experiments. It can be shown that this method has an error of less than 6% in determining the vibration amplitude when the amplitude is below 30 nm.

### 3. Experimental Setup

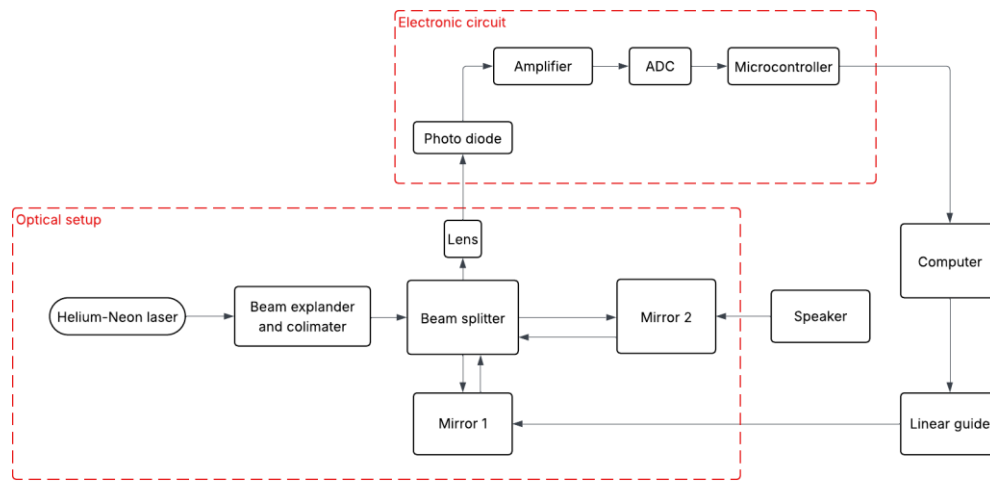


**Figure 4.** Block diagram of the implemented setup

As depicted in Fig. 4, the experimental setup consists of two main components: the optical setup and the electronic circuit.

#### 3.1 Optical setup

The optical setup follows the configuration of a standard Michelson interferometer. The light source is a helium–neon laser with a wavelength of 632.8 nm. The output beam passes through a beam expander and collimator, which expand and collimate the laser beam. This expanded beam is then split into two coherent beams by a beam splitter. Each beam is reflected by a mirror: one mirror is mounted on a linear guide for precise position adjustment (Fig. 6), while the other mirror is vibrated using a speaker. The mirror attached to the linear guide is also used to monitor the vibrations induced by the linear guide motor.



**Figure 5.** Optical setup mounted on a granite surface with dampers.

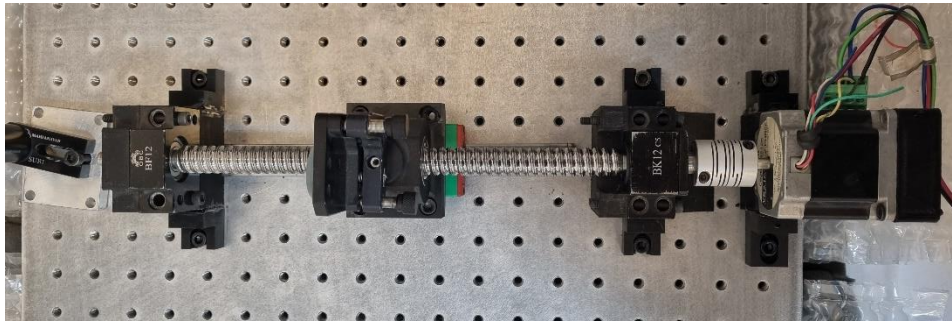


Figure 6. Linear guide for controlling the precise position of the mirror.

### 3.2 Electronic circuit

The electronic circuit, depicted in Fig. 7, consists of a photodiode, an amplifier, an analog-to-digital converter (ADC), and a microcontroller. The photodiode detects changes in light intensity within the interference pattern caused by mirror vibrations. The resulting analog signal is amplified and then digitized by the ADC. The microcontroller captures the digital data from the ADC and transmits it to a computer for further processing.

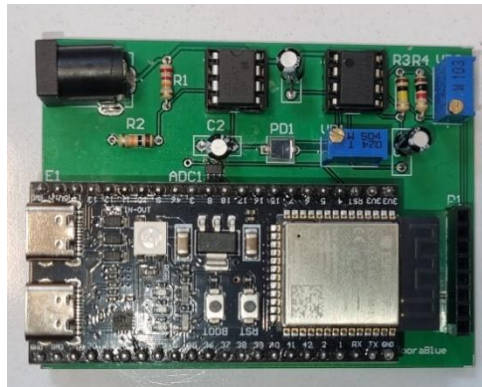


Figure 7. Electronic circuit implemented for capturing light intensity and transferring data to computer

## 4. Experiments and Results

We conduct several experiments to test the implemented vibration measurement system and demonstrate the results obtained for each experiment.

### 4.1 Detection of single-tone sinusoid vibration

A single-tone sound with a frequency of 1008Hz was played through the speaker, the intensity signal from the electronic circuit was captured and converted to vibration using Eq. (5). Fig. 8(a) and Fig. 8(b) show the measured mirror vibration in time and frequency.

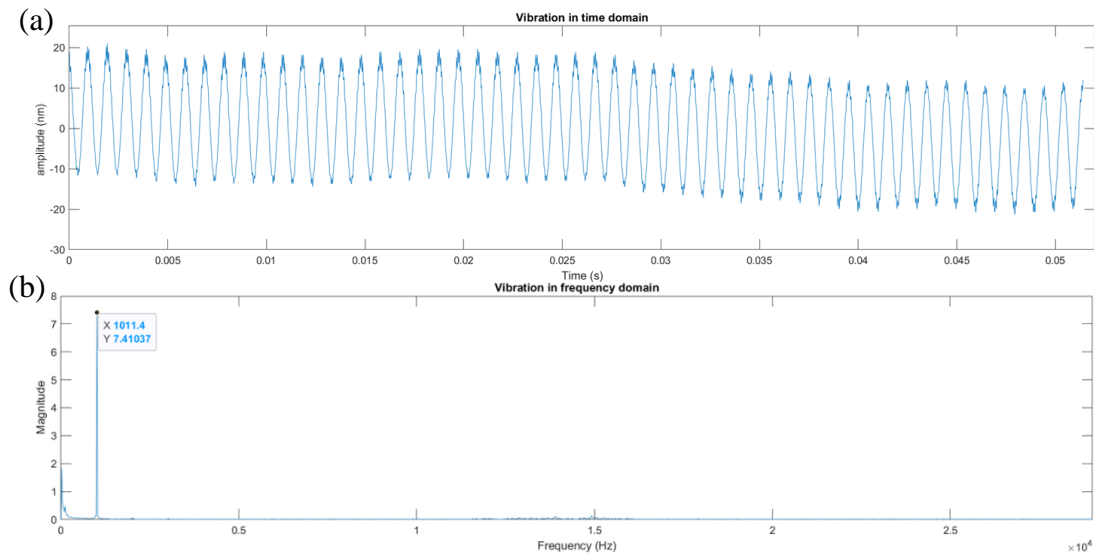


**Figure 8.** Vibration of mirror for a 1008Hz single-tone input

(a). In time domain      (b). In frequency domain

As shown in Fig. 8, the vibration has an amplitude of around 15nm and estimated frequency is approximately 1011.4 which is very close to the frequency of the vibration source.

#### 4.2 Detection of single-tone sinusoid vibration with mirror at a distance

In this experiment we repeated the same procedure in last section but with the mirror at a distance of few meters from the setup, this is important because it shows that this setup can be used to measure vibrations of structures that are not close to our measurement setup and we don't have a direct access to them.

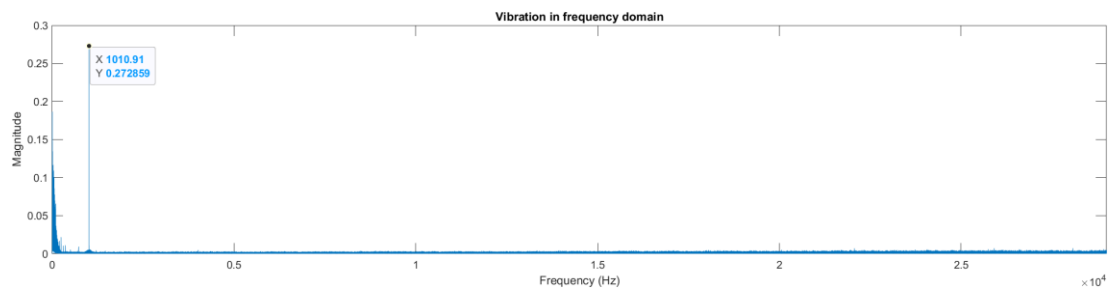


**Figure 9.** Vibration of mirror for a 1008Hz single-tone input in frequency domain

As shown in Fig. 9, the estimated frequency for the vibration is around 1010.9Hz which is very close to the source frequency. Note that in this experiment the mirror is not on the optical breadboard which other optical instruments are mounted on it and this has resulted in a greater noise due to the vibration of environment.

#### 4.3 Finding the resonance frequency of optical setup as a mechanical structure

In this experiment, we model the entire optical setup as a mechanical structure with resonant frequencies. When a vibration is applied at a frequency matching one of these resonances, the system responds with significantly larger amplitude compared to vibrations at other frequencies. To determine the resonance frequency, we apply a mechanical tap to a specific part of the optical breadboard. This tap acts as an impulse excitation, producing a broad frequency spectrum that excites all the natural modes of the structure [5], [6]. Vibrations with frequencies close to the system's resonance persist longer due to reduced damping, and in the frequency-domain response, these resonances appear as distinct peaks [7]. Fig. 10(a) and Fig. 10(b) show the impulse response of the system in time and frequency domain.

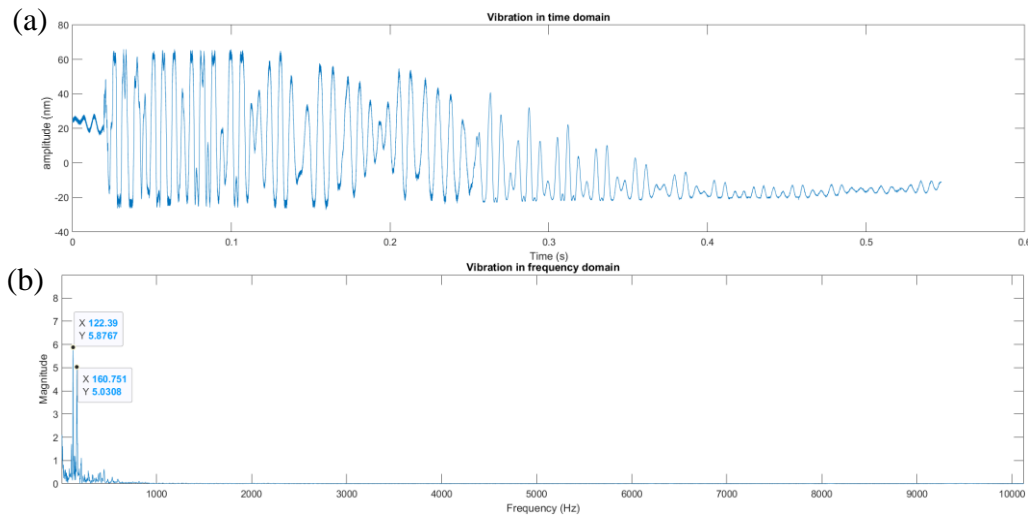


**Figure 10.** Impulse response of the system, (a). In time domain (b). In frequency domain

The frequency response shown in Fig. 10(b) suggests that 122 Hz and 161 Hz are potential resonance frequencies of the system. To verify this, we applied single-tone sinusoidal vibrations at various frequencies, including 122 Hz and 161 Hz, using a speaker. By analyzing the peaks of the vibration signals in the frequency domain at each stimulated frequency, we identified the frequencies at which the system exhibited the strongest response. The speaker was mounted at the same location on the optical breadboard as in the previous impulse excitation test, ensuring consistent excitation conditions. Table 1 presents a comparison of the vibration amplitudes at 100 Hz, 113 Hz, 122 Hz, 161 Hz and 337Hz. As shown, the system's response at 161 Hz and 122Hz are significantly greater than at the other frequencies, indicating that they are the resonant frequencies of the system.

**Table 1.** Comparing the peak magnitude for different stimulated frequencies.

Stimulated frequency (Hz)	Peak magnitude (nm)
100	0.07
113	0.24
122	19.77
161	20.46
337	4.75

#### 4.4 Detection of vibrations due to the sound of music and reconstructing music

The system has demonstrated reliable performance in detecting single-tone vibrations generated by the speaker. To verify its capability to detect a broad range of frequencies while preserving signal integrity, we played a music track through the speaker attached to the mirror and recorded the resulting vibration signal. Figure 11 presents a segment of the captured vibration waveform induced by the music. By using the sound function in MATLAB to play back the recorded vibration signal, we were able to audibly reproduce the original music played by the speaker.<sup>1</sup> (Note that the recorded signal is raw and unfiltered. Its quality can be enhanced through hardware and software filtering)

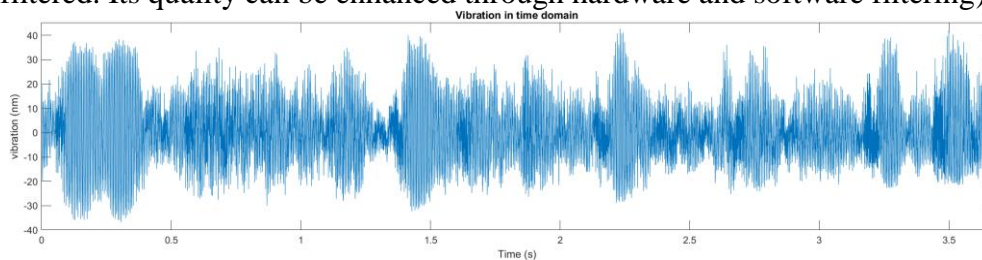


**Figure 11.** Recorded vibration for a music input

<sup>1</sup> Listen to the reproduced music at: <https://drive.google.com/file/d/1rM7x3FwZxpESbXtHGHQ7Ebv5U5e59fYv/view?usp=sharing>

#### 4.5 Detection of vibration of motor

One important factor in a linear guide system used for precision linear motion is motor-induced vibration. Such vibration can reduce the resolution of an imaging system, as it causes unwanted motion of the object being imaged [8]. To assess whether the designed system can measure motor-induced vibration in a practical setup, we employed the linear guide shown in Fig. 5 to record the vibration of the mirror when the motor was powered on but not in motion.

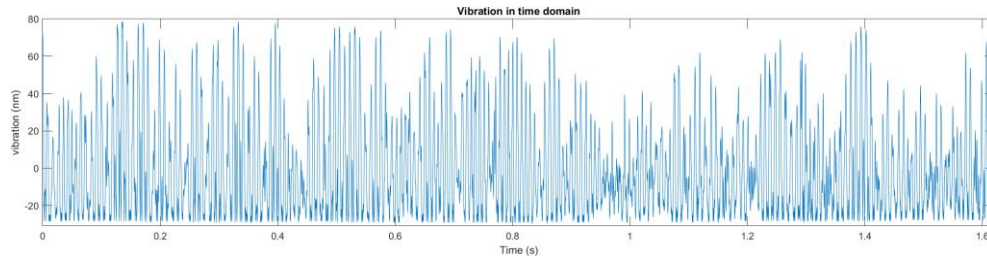


Figure 12. Vibration due to motor in a linear guide system

### 5. Conclusion

In this paper we presented a precise vibration measurement system based on Michelson interferometer. The system was successful in measuring vibrations with nanometer order precision. The sampling frequency of the system is around 58kHz which can theoretically be used to detect frequencies up to 29kHz based on Nyquist theorem, which enables the system to measure vibrations with a wide range of frequencies. The advantage of our system compared to other similar optical instruments is its simple and low-cost implementation, which makes it accessible for a wide range of laboratory and industrial uses. This system can be a solution to various real world problems like precise stability measurement of mechanical systems and detection of structural resonances. Future work may focus on designing a phase stabilizer to maintain linearity of the system, improving environmental noise rejection, and integrating it into compact, portable platforms for field use.

### REFERENCES

1. Saidin, S.S., Jamadin, A., Abdul Kudus, S. et al. An Overview: The Application of Vibration-Based Techniques in Bridge Structural Health Monitoring. *Int J Concr Struct Mater* 16, 69 (2022).
2. Y.-H. Shin, S.-J. Moon, Y.-J. Kim, K.-Y. Oh, "Vibration control of scanning electron microscopes with experimental approaches for performance enhancement", *Sensors* 20, 2317 (2020).
3. Huang, G.; Cui, C.; Lei, X.; Li, Q.; Yan, S.; Li, X.; Wang, G. A Review of Optical Interferometry for High-Precision Length Measurement. *Micromachines* 2025, 16, 6.
4. B. E. A. Saleh and M. C. Teich, *Fundamentals of Photonics*, 3rd ed. Hoboken, NJ, USA: Wiley, 2019.
5. Ryu S, Kim SC. Knocking and Listening: Learning Mechanical Impulse Response for Understanding Surface Characteristics. *Sensors (Basel)*. 2020 Jan 9;20(2):369. doi: 10.3390/s20020369. PMID: 31936449; PMCID: PMC7013596.
6. Brown, David L., and William G. Halvorsen. "Impulse technique for structural frequency response testing." *Sound and Vibration* 11.11 (1977): 8-21.
7. D. J. Ewins, *Modal Testing: Theory, Practice and Application*, 2nd ed. Baldock, UK: Research Studies Press, 2000.
8. Tian N, Jiang H, Xue L and Xie J (2022) Influence of Photon Beam and Motor Vibrations on At-Wavelength X-Ray Speckle Scanning Metrology. *Front. Phys.* 10:864985. doi: 10.3389/fphy.2022.864985